PHILOSOPHICAL TRANSACTIONS OF THE ROYAL SOCIETY A MATHEMATICAL, PHYSICAL & ENGINEERING SCIENCES

Substorm Processes in the Geomagnetic Tail and their Effect in the Nightside Auroral Zone Ionosphere as Observed by EISCAT [and Discussion]

P. J. S. Williams, T. S. Virdi, S. W. H. Cowley, M. Lockwood, P. Rothwell and K. J. Winser

Phil. Trans. R. Soc. Lond. A 1989 **328**, 173-193
doi: 10.1098/rsta.1989.0030

Phil. Trans. R. Soc. Lond. A **328**, 173–193 (1989)
Printed in Great Britain

Substorm processes in the geomagnetic tail and their effect in the nightside auroral zone ionosphere as observed by EISCAT

BY P. J. S. WILLIAMS[1], T. S. VIRDI[1] AND S. W. H. COWLEY[2]

[1] *Department of Physics, University College of Wales, Aberystwyth, Dyfed SY23 3BZ, U.K.*
[2] *Blackett Laboratory, Imperial College, London SW7 2BZ, U.K.*

[Plates 1 and 2]

Current understanding of magnetospheric substorms is reviewed with special emphasis on the relation between space-based and ground-based observations. It is pointed out that the traditional means of monitoring substorms from the ground (by using magnetometers, riometers and auroral observations) give only a selective picture of the whole phenomenon, related to the precipitation of electrons with energies above 1 keV. Measurements by incoherent scatter radar, such as the European incoherent scatter facility (EISCAT), give a more complete and continuous picture.

The 'neutral line' model of substorms provides a natural, physical basis on which relevant data can be interpreted. In this picture, two sources of flow are anticipated in the nightside auroral zones, one 'directly driven' (with a delay of 15–20 min) by the interplanetary magnetic field (IMF) B_z component and associated with dayside reconnection, and the other appearing typically an hour after southward turnings of the IMF and associated with rapid tail reconnection during substorms. Evidence for the influence of both sources of flow is found in nightside EISCAT data. These data also reveal that, overall, the nightside ionospheric flow and plasma parameters often vary in a quasi-periodic way with a period of *ca.* 1 h. In two cases in which concurrent interplanetary data are available it appears that the periodicity is inherent in IMF B_z, but this is not expressed unmodified in the auroral zone because of the presence of the two sources of flow which depend on IMF B_z in different ways.

1. INTRODUCTION

The magnetospheric substorm is a dynamic global phenomenon involving an immense volume of space, from the dayside magnetopause to the distant geomagnetic tail. It also involves a diverse range of linked physical processes which are understood in varying degrees of completeness, such as magnetic reconnection, both at the magnetopause and in the tail, plasmoid formation, plasma acceleration and injection into the radiation belts, auroral electron acceleration and precipitation, and ionospheric electrojet excitation. To fully comprehend the relations which exist between these processes, preplanned multipoint observations of key regions of the system are ideally required, using both spacecraft and ground-based facilities. However, although this has yet to be fully achieved, much has been learned over the past two decades both from case studies of multipoint data mainly obtained serendipitously, and from analyses of single point data, often combined with data from geomagnetic observatories in the form of disturbance indices, and from spacecraft in the solar wind monitoring interplanetary conditions (see, for example, the reviews by Baker *et al.* (1984*b*) and Baumjohann (1986), and references therein).

In §2 we give a brief review of events during a simple isolated substorm as revealed by these observations, with particular emphasis on the relation between effects seen in space and on the ground. The observations will be interpreted in terms of the current widely accepted paradigm which involves energy storage in the geomagnetic tail, followed by its release in association with the formation of a near-Earth neutral line. Other interpretations have recently been forwarded by Rostoker & Eastman (1987), but will not be discussed here. A critique has been presented by Baumjohann (1988). Section 3 then discusses the limitations of the traditional ground-based monitors of geomagnetic activity, and the power of the new generation of incoherent scatter radars such as the European incoherent scatter facility (EISCAT). Finally in §4 we present some recent EISCAT observations which bring out a new facet which has not previously been clearly recognized, that the ionospheric flow effects which are related to geomagnetic disturbance, and associated ionospheric parameter changes, are often quasi-periodic in nature with periods between 30 and 60 min.

2. The magnetospheric substorm

In this section we shall describe the sequence of events which occur during a simple isolated substorm. Observations show that such a substorm can be described in terms of three phases, growth, expansion and recovery, each lasting typically for an interval of many tens of minutes (McPherron 1970, 1972, 1979; McPherron *et al.* 1973). The magnetosphere is supposed initially to be in a quiescent state with relatively weak internal convection (corresponding to a cross-magnetosphere voltage of a few tens of kilovolts), possibly driven by some form of 'viscous' interaction at the boundary. Under such circumstances the tail neutral line is believed to lie in the more distant tail, at distances of *ca.* 100–200 R_E† from Earth (Slavin *et al.* 1985; Richardson *et al.* 1989). The substorm growth sequence then begins with a sharp southward turning of the interplanetary magnetic field (IMF), which immediately results in a substantial increase in the rate of reconnection, and open flux production, at the dayside magnetopause (Rijnbeek *et al.* 1984; Paschmann *et al.* 1986). The newly formed open tubes are then carried by the magnetosheath flow from the dayside to the nightside of the magnetosphere, such that the closed flux on the dayside is reduced and the magnetopause moves inwards, typically by *ca.* 1 R_E (Aubry *et al.* 1970; Fairfield 1971; Holzer & Slavin 1978), while the flux in the tail lobes is increased. In the near-Earth tail the flaring angle of the tail magnetopause becomes larger, so that the field strength of the tail lobe is also increased, while in the more distant tail, where flaring remains small, the tail instead expands in radius (Maezawa 1975; Baker *et al.* 1984*a*, 1987*a*, *b*; Fairfield *et al.* 1989).

In the ionosphere, the magnetic stresses exerted on the newly opened flux tubes, located adjacent to and equatorward of the pre-existing polar cap, excite an enhanced twin-vortex flow at high latitudes, which expands with the new patch of open flux at speeds of several kilometres per second (Rishbeth *et al.* 1985; Lockwood *et al.* 1986). In the noon sector at high latitudes these flows are observed within a few minutes (less than *ca.* 5 min) of the arrival of southward fields at the subsolar magnetopause, the delay increasing to *ca.* 10 min near the dawn–dusk meridian (Etemadi *et al.* 1988; Todd *et al.* 1988), and to *ca.* 15–20 min on the nightside (Baker *et al.* 1985; Bargatze *et al.* 1985). The dayside values were determined from direct observations of ionospheric flows by the EISCAT radar, while the nightside values were obtained from analysis

† $R_E = 6.37 \times 10^6$ m.

PHILOSOPHICAL TRANSACTIONS OF THE ROYAL SOCIETY A MATHEMATICAL, PHYSICAL & ENGINEERING SCIENCES

of the geomagnetic disturbance produced by the corresponding ionospheric polar-disturbance (DP2) current system (Nishida 1968*a*, *b*). As the amount of open flux in the polar cap grows, its area expands, and with it the radius of the bordering auroral oval (Vorobjev *et al.* 1976; Holzer *et al.* 1986). The expansion speed of the oval is typically a few hundred metres per second (corresponding to an applied voltage at the dayside magnetopause of *ca.* 100 kV), which we note is about an order of magnitude slower than the initial expansion speed of the new flow pattern itself.

During the substorm's growth phase, therefore, part of the input of energy from the solar wind is fed into atmospheric heating by means of ionospheric Pedersen currents, in an essentially directly driven fashion, while the remainder is stored in the magnetic field of the tail lobes. In the nightside magnetosphere the latter storage results in the magnetic field becoming increasingly distorted from a dipolar orientation, even as close to the Earth as geostationary orbit (6.6 R_E) (McPherron 1970), thus in turn producing characteristic changes in the pitch angle distributions of trapped radiation-belt particles (Baker *et al.* 1978, 1979, 1982, 1985). At somewhat larger distances (*ca.* 15–20 R_E), the plasma sheet is observed to thin (Buck *et al.* 1973; Kivelson *et al.* 1973) while the magnetic flux threading it decreases (Fairfield 1986), the plasma and embedded flux presumably convecting inwards towards the Earth as enhanced magnetospheric circulation is excited.

At some stage in this process, however, the magnetic field in the near-Earth tail undergoes a rapid reconfiguration, usually after a growth phase lasting between 30 and 60 min, with the results shown in figure 1. At this time, corresponding to the onset of the substorm expansion phase (figure 1*a*), a new neutral line is believed to form in the near-Earth plasma sheet (usually between 10 and 20 R_E from the Earth), in a restricted local time sector near midnight where the plasma sheet is thinnest (Russell & McPherron 1973; Hones 1973, 1979). The details of the physical processes leading to the field reconfiguration are, however, unclear. In some substorms the change appears to be externally triggered, either by a sudden change in the dynamic pressure of the solar wind (Kokubun *et al.* 1977), or by a sudden northward turn of the IMF (Caan *et al.* 1978; Rostoker 1983), though many substorm expansion onsets occur under rather steady interplanetary conditions (Horwitz 1985), such that an internal instability is indicated (Schindler 1974; Galeev *et al.* 1978).

In either case, reconnection at the new neutral line initially forms closed loops of magnetic flux within the plasma sheet which are surrounded by closed plasma sheet flux tubes connected to the Earth at either end (figure 1*a*). However, the rate of reconnection at the new neutral line is sufficiently large that after a few minutes all the closed tubes in this local time sector pass through the separatrix, and open tail lobe tubes begin to be reconnected. Consequently, the pre-existing plasma sheet tailward of the new neutral line becomes disconnected from the Earth, forming a closed-loop plasmoid which is surrounded by an increasingly thick layer of disconnected 'interplanetary' flux. The plasmoid is propelled down the tail away from the Earth by the stress of this surrounding flux, and by the dynamic pressure of the accelerated tailward-flowing plasma tailward of the new neutral line, reaching speeds of *ca.* 600 km s^{-1}, comparable to the speed of the latter plasma. Consequently, the plasma which is accelerated tailward of the new neutral line is mainly confined to a thin wedge-shaped region earthward of the retreating plasmoid, termed the post-plasmoid plasma sheet (the PPPS in Figure 1*b*, 1*c*) (Richardson & Cowley 1985; Richardson *et al.* 1987*b*). Near-Earth observations which relate to plasmoid release, and the subsequent formation of a thin tailward-jetting PPPS, have been

PHILOSOPHICAL TRANSACTIONS OF THE ROYAL SOCIETY A MATHEMATICAL, PHYSICAL & ENGINEERING SCIENCES

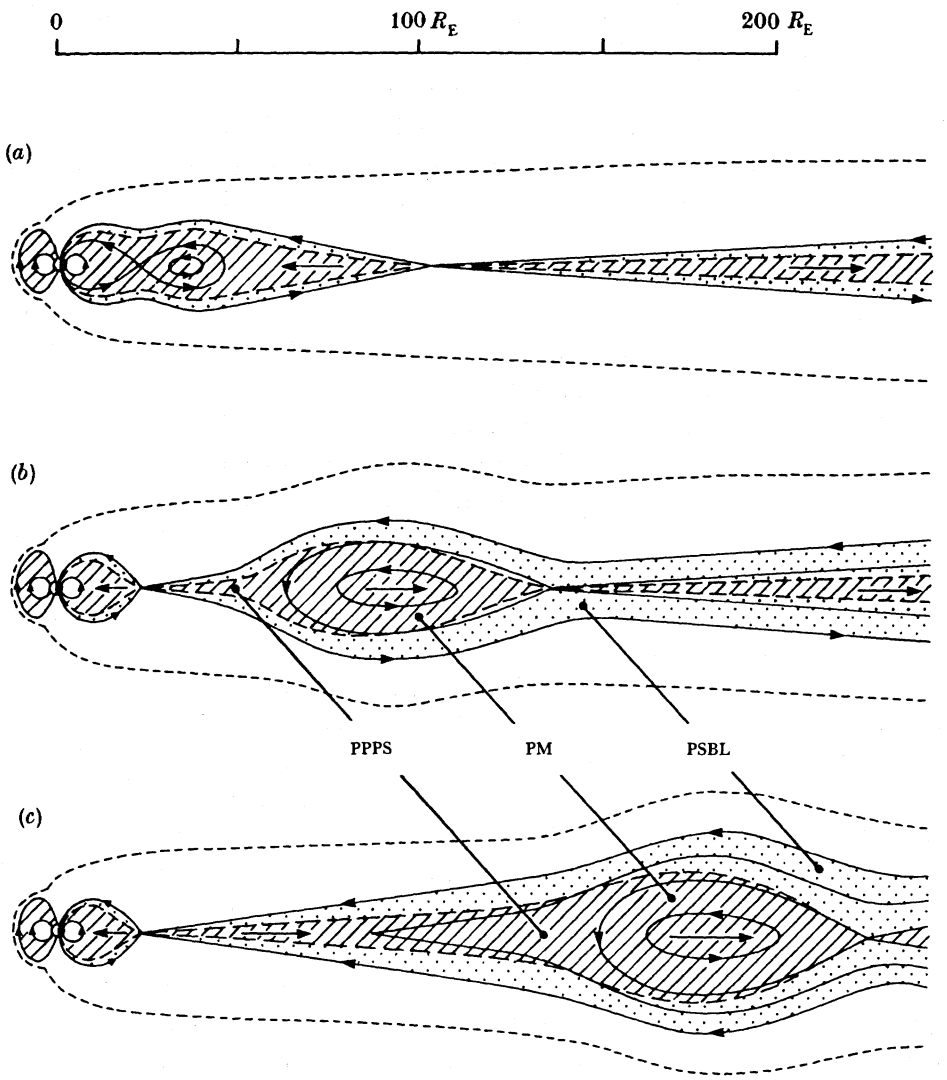

FIGURE 1. Sketches of the geomagnetic tail (noon–midnight cross section) illustrating the formation and downtail propagation of plasmoids, according to the neutral line model of substorms. Solid lines are magnetic field lines, the hatched areas bounded by dashed lines indicate the $\beta \gg 1$ 'plasma sheet' regions (in particular the plasmoid (PM) and postplasmoid plasma sheet (PPPS)), and the dotted regions lying between the plasma sheet boundary (dashed line) and the field separatrices mapping to the neutral lines are the plasma sheet boundary layers containing streaming energetic particles (after Richardson *et al.* 1987*b*).

presented by Hones (1973, 1979), Nishida & Nagayama (1973), Hones *et al.* (1976), Coroniti *et al.* (1980), Fairfield *et al.* (1981) and Bieber *et al.* (1982). In the distant tail (*ca.* 100–200 R_E from Earth), well-developed plasmoid structures have been observed travelling downtail following substorm onsets, providing further strong evidence in support of this picture (Hones *et al.* 1984*a*, *b*; Scholer *et al.* 1984*a*, *b*; Richardson & Cowley 1985, 1987; Richardson *et al.* 1987*b*).

Earthward of the neutral line, however, the reconnected flux tubes collapse towards the Earth under the action of the magnetic stress, resulting in a return of the distorted field to a more dipolar form (Cummings *et al.* 1968; Lopez *et al.* 1988). This collapse propagates as a sharply defined wave, which moves in towards the Earth at speeds up to *ca.* 100 km s^{-1} near

to geostationary orbit (Moore *et al.* 1981; Arnoldy & Moore 1983). At each location earthward of the neutral line the field change is therefore abrupt, but occurs at later times successively closer to the Earth. Large inductive electric fields accompany this 'dipolarization' of the magnetic field, which are consistent with a rapid inward motion of the flux tubes near the equatorial plane, and a rapid outward motion at higher latitudes, as expected (Pedersen *et al.* 1978; Shepherd *et al.* 1980; Aggson *et al.* 1983). As the tubes collapse, the plasma they contain is compressed and heated, such that the change in the field is also accompanied by a dispersionless (in energy) injection of hot tail plasma into the outer radiation zone (ring current region) (Arnoldy & Chan 1969; Baker *et al.* 1978; Sauvaud & Winckler 1980; Lopez *et al.* 1988), and a prompt expansion of the near-Earth plasma sheet (McPherron *et al.* 1973; Pytte *et al.* 1976*b*). The field change is sufficiently rapid that the second adiabatic invariant of the thermal ions is violated, the ions being accelerated to form field-aligned beams which expand away from the equator on either side, and then bounce back and forth on the closed flux tubes (Quinn & McIlwain 1979; Quinn & Southwood 1982; Mauk 1986). Subsequently, the injected plasma undergoes energy-dependent drifts in the quasi-static fields of the inner magnetosphere, producing complex dispersion patterns (DeForest & McIlwain 1971; Mauk & Meng 1983).

At low altitudes, the onset of the expansion phase is marked by a sudden brightening of the aurora in the equatorward portion of the region of discrete forms (Akasofu 1964). This occurrence may relate to the onset of rapid reconnection at the new substorm neutral line before plasmoid disconnection (figure 1*a*), though the physical details of this possible connection remain unclear (see, for example, Atkinson *et al.* 1988). The onset is also marked by a burst of Pi2 pulsations (Morozumi 1965; Rostoker 1968; Saito 1969), which appear to relate to a *ca.* five-minute burst of low-frequency magnetic fluctuations observed in the near-Earth plasma sheet following 'dipolarization', earthward of the neutral line (Pytte *et al.* 1976*b*). After the plasmoid has become disconnected from Earth, the new neutral line becomes connected to the poleward border of the auroral oval. As the reconnection of open tail lobe flux tubes then proceeds, a patch of newly closed flux will grow in the ionosphere, expanding polewards from the pre-existing boundary in a strip corresponding to the local time sector of the neutral line. Precipitation of the hot plasma contained on these flux tubes (modified at higher latitudes by field-aligned voltages associated with field-aligned currents) will then result in a corresponding poleward expansion of the aurora, which typically takes place at speeds of several hundred metres per second (Craven & Frank 1987). As in the case of dayside reconnection discussed above, the change in the nightside field configuration brought about by tail reconnection will also tend to excite an expanding pattern of twin-vortex flow in the ionosphere, associated with an equatorward (as well as east–west) flow within the expanding strip and an ionospheric electric field with a westward-directed component. However, subsequent developments are complicated by the fact that the auroral precipitation strongly enhances the electrical conductivity within the strip compared with the surrounding region of the nightside ionosphere, with the Hall conductivity generally being large compared with the Pedersen conductivity, since the kiloelectronvolt-electron precipitation into the strip produces ionization preferentially at E-region heights (Baumjohann *et al.* 1981; Inhester *et al.* 1981). In particular, the westward electric field associated with the equatorward flow will result in a westward Pedersen current flow along the strip, and a much larger Hall current flow across the strip directed northward. Because of the inhomogeneity of the conductivity, the ionospheric

PHILOSOPHICAL TRANSACTIONS OF THE ROYAL SOCIETY A MATHEMATICAL, PHYSICAL & ENGINEERING SCIENCES

currents flowing in the strip must largely close in the magnetosphere, via line-like field-aligned currents (FAC) flowing from its ends, and sheet-like currents flowing on the northern and southern borders of the strip. However, the ability of the magnetosphere to close the latter currents appears to be limited, and instead a southward polarization electric field is developed whose Pedersen current largely cancels the northward Hall current. This requires the southward field to be larger than the initial westward field by approximately the Hall-to-Pedersen conductivity ratio. In turn, the southward electric field produces a large westward Hall current flowing along the strip which augments the westward Pedersen current by a factor of approximately the square of the Hall-to-Pedersen conductivity ratio, i.e. by about an order of magnitude. The total westward (Cowling) current constitutes the substorm westward electrojet, which closes by means of a downward FAC at its eastward end, and an upward FAC at its westward end (Bostrom 1964, 1974). These FACs correspond to the magnetic field shear between the central region of collapsed 'dipolarized' field lines lying downstream from the neutral line, and the tail-like fields which remain to the east and the west, the FAC eventually feeding into the equatorial current sheets of the latter regions. The electrojet–FAC system so produced is usually referred to as the 'substorm current wedge' (McPherron *et al.* 1973; Clauer & McPherron 1974; Singer *et al.* 1985; Nagai 1987), and is often described as resulting from a 'short-circuit' or 'diversion' of the cross-tail current from the central tail into the ionosphere, though as discussed here, it may also be viewed as a direct and natural consequence of the azimuthally localized field collapse following tail reconnection.

As the expansion phase proceeds, however, it is clear that the substorm neutral line must generally expand to the east and west across the tail, though not always in a continuous fashion (Arnoldy & Moore 1983; Nagai *et al.* 1983). An expansion in the width of the field collapse, substorm current wedge and auroral 'bulge' then follows. In particular, the region of upward field-aligned current located at the expanding westward end of the electrojet corresponds to the 'westward-travelling surge'(WTS). However, many substorms have multiple onsets at intervals of 10–20 min, each associated with an auroral brightening and WTS, a Pi2 burst, an intensification of the westward electrojet, and an expansion of the plasma sheet in the near-Earth tail, earthward of the neutral line (Clauer & McPherron 1974; Pytte *et al.* 1976*a*, *b*; Nagai *et al.* 1983). Each surge in activity tends to carry the disturbance further to the east and west about an onset centred usually in the midnight sector. These observations suggest that periodic enhancements of the tail reconnection rate, and expansions in the east–west extent of the neutral line, are involved in multiple-onset substorms, though it is not known whether these take place as developments of the neutral line system formed at the initial onset, or whether they are associated with the formation of a new neutral line and the production of a further plasmoid. Richardson *et al.* (1987*a*) have recently presented evidence in favour of the latter picture, though the number of cases examined so far is very few.

Finally, after about an hour the auroral 'bulge' reaches its maximum extension, and both the discrete auroras at its poleward border (mapping to the vicinity of the neutral line and plasma sheet boundary layer), and the diffuse aurorae at lower latitudes (mapping to the 'injected' hot plasma in the inner magnetosphere) begin to fade, marking the beginning of the substorm recovery phase. Recovery normally (but not invariably) starts after the near-Earth tail lobe field has returned substantially to pre-growth-phase values. The substorm neutral line then undergoes a rapid retreat into the more distant tail, resulting in the expansion of the near-Earth plasma sheet back to its quiet-time thickness (Hones *et al.* 1971, 1973; Lui *et al.* 1975), though the precise conditions that lead to this rapid change are far from clear.

PHILOSOPHICAL TRANSACTIONS OF THE ROYAL SOCIETY A MATHEMATICAL, PHYSICAL & ENGINEERING SCIENCES

In summary, therefore, during the expansion phase of the substorm the solar wind energy stored in the magnetic field of the tail lobes during the growth phase is released. Much of this energy is actually returned to the solar wind via the plasmoid and fast plasma flows that occur tailward of the neutral line. The remainder is fed into Joule heating of the atmosphere, and into the hot plasmas which are accelerated earthward of the neutral line and injected into the inner magnetosphere. The latter energy reservoir is dissipated by precipitation into the atmosphere, by charge-exchange of ions with the hydrogen geocorona producing energetic escaping neutrals, and by escape from the magnetopause. However, the fact that energy is released from the tail during the substorm does not preclude the possibility that processes that are directly driven by the solar wind may simultaneously be present, which might considerably influence the progress of the substorm itself. In fact these effects must occur if intervals of southward interplanetary field and dayside reconnection continue to be present during the substorm, which will inevitably lead to direct modulation of the ionospheric flow and Joule dissipation, and flux addition to the tail. Considerable variations in behaviour from interval to interval are therefore to be expected. Indeed, during intervals of strong, continuous, southward interplanetary fields it appears that the magnetosphere may enter a state of strong continuous disturbance in which dayside and nightside reconnection rates are approximately in balance, and upon which weak substorm-like features are only intermittently superposed (Pytte *et al.* 1978). Richardson *et al.* (1989) have recently presented evidence that the neutral line may remain continuously within the cislunar tail during such intervals, and that some of the disturbance enhancements may be related to an enhancement of the reconnection rate at an existing neutral line, rather than being as a result of the formation of new neutral lines and plasmoids.

3. Ground-based measurements of substorms

As indicated in the above discussion, during a magnetospheric substorm a large amount of energy originating from the solar wind is dissipated in the high-latitude ionosphere by the Joule heating associated with Pedersen currents. Energy input to the ionosphere also takes place in the form of charged particle precipitation from the plasma populations accelerated during the substorm, but present estimates suggest that this input represents less than 10% of the total energy, as shown in figure 2 where the total Joule heating is compared with the total particle heating for the period 15h40 to 22h00 U.T. on 18 October 1985 (Schlegel & McCrea 1987). The importance of precipitation lies in the secondary ionization produced in the ionosphere, which in the nightside auroral zone will have a profound influence on the ionospheric conductivity and hence dissipation rate. However, the Hall and Pedersen conductivities can be enhanced to differing degrees relative to each other depending on the energy of the precipitating electrons, because the Pedersen conducting layer lies above the Hall layer, and the height range in which precipitating electrons produce ionization depends upon their energy. Consequently, the Pedersen conductivity of the ionosphere, and the major dissipation process, depends upon the influx of lower-energy electrons, below *ca.* 1 keV, while the Hall conductivity depends upon the influx of higher-energy electrons, between *ca.* 1 and *ca.* 10 keV. It is therefore important to emphasize that the ground-based techniques which have traditionally been used to monitor magnetospheric activity, and which have contributed to the development of the picture presented in the last section, predominantly monitor the effects produced by the more energetic electron precipitation, and are insensitive to the main energy transfer between the magnetotail and ionosphere by means of Joule heating. Specifically,

PHILOSOPHICAL TRANSACTIONS OF THE ROYAL SOCIETY A MATHEMATICAL, PHYSICAL & ENGINEERING SCIENCES

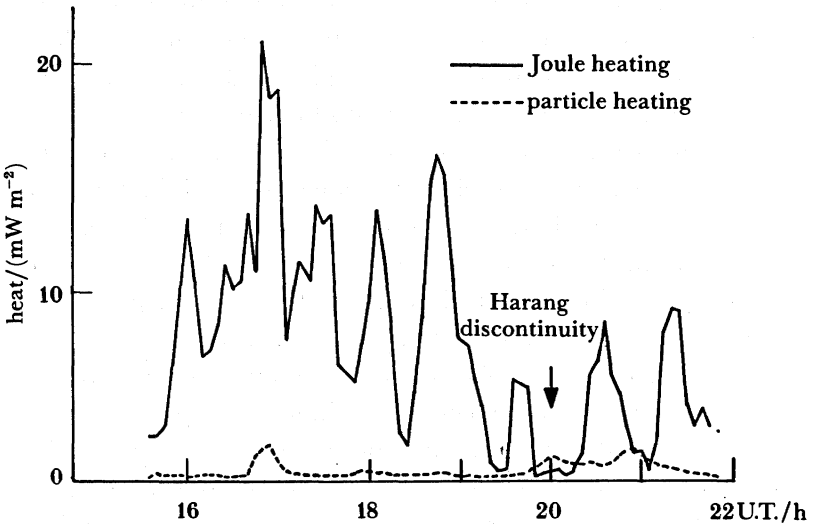

FIGURE 2. Total Joule heating and particle heating as measured by EISCAT on 18 October 1985.

riometers, which measure the ionospheric absorption of galactic radio noise at 30 MHz, are sensitive to the precipitation of 20–50 keV electrons, all-sky cameras and photometers, which record auroral light emission, are mainly sensitive to 5–20 keV precipitation, while ground-based magnetometers mainly record the variations of ionospheric Hall rather than Pedersen currents, because the latter are largely solenoidal in nature and produce little magnetic signature on the ground.

This major deficiency in the study of substorm energy can be overcome by the use of incoherent scatter radars, such as the EISCAT facility recently set up in northern Scandinavia (Folkestad *et al.* 1983). The EISCAT ultra-high-frequency (UHF) radar, data from which is to be presented in the next section, is a tristatic system with a transmitter at Tromsø and receiving systems at Tromsø, Kiruna and Sodankylä. By virtue of its location it is ideally suited to the study of nightside auroral phenomena, and its design as a 'second-generation' radar also allows measurement of an unprecedented range of ionospheric parameters. Data from Tromsø allow the routine derivation of the height (or more generally, range) profiles of the electron density N, electron and ion temperatures T_e and T_i, and the line-of-sight ion velocity. Measurements made at Kiruna and Sodankylä then provide the other two components of the full velocity vector V_i, as long as the signal-to-noise ratio for the signals they receive is sufficiently high.

From these basic parameters a variety of other quantities may be determined. The electric field $\boldsymbol{E}$ transverse to the magnetic field can be obtained from F-region measurements of V_i, since the field-perpendicular flow in that region is just the $\boldsymbol{E}\times\boldsymbol{B}$ drift. By combining the height profiles of N with a collision-frequency profile obtained from a suitable neutral atmosphere model, the Hall and Pedersen conductivities can also be obtained, and hence the Joule heating rate from a further combination of the latter quantity with $\boldsymbol{E}$. The density and temperature measurements also give direct information about the local precipitation of electrons into the ionosphere. In particular, in the ionospheric D- and E-regions the ion–electron recombination time is 2 min or less, so that variations in N at a given height reflect similar variations in the rate of ionization. Such variations could arise from changes in either the flux or the mean energy of the precipitating electrons, but these can be separated out by deconvolving the height

profile (Banks 1977), so that the precipitating electron energy spectrum can be determined at energies above *ca.* 1 keV. Lower-energy electrons deposit their energy at higher altitudes where the recombination time is longer, typically an hour or more in the F-region, so that the measurements of N are not sensitive to the local 'soft' electron precipitation. However, the precipitation does cause an increase in T_e, from which the precipitating electron flux below *ca.* 1 keV can be estimated by equating the input of energy to the electron population to the rate of cooling at the enhanced temperature (Schunk & Nagy 1978). In the next section we shall display variations of F-region electron temperatures and E-region electron densities determined by the EISCAT radar as simple indicators of the variations of the 'soft' and 'harder' (greater than 1 keV) electron precipitation, respectively.

As mentioned above, the EISCAT UHF system is tristatic, and thus has the unique advantage of providing a value of $\boldsymbol{v}_i$ that is free from systematic error, even when the plasma velocity varies rapidly in time and space. However, the tristatic method cannot always be used, because of low signal-to-noise at Kiruna and Sodankylä, leading to large random errors in V_i. In such a case the Tromsø antenna can be pointed in three non-planar directions in quick succession, and the line-of-sight velocities combined to produce a flow vector, assuming that V_i is constant in space and time over the cycle. If this assumption is valid, which will not always be the case during substorms, the monostatic mode can provide V_i with far smaller noise errors than the tristatic mode, especially when measurements made at different heights are combined (Williams *et al.* 1984; Jones *et al.* 1986).

At extreme ranges from Tromsø the signal-to-noise ratio is even lower, and the problem of determining the full vector of velocity by the tristatic method is compounded by the unfavourable geometry of the system as the line-of-sight directions from the scattering volume to the three receiving sites are closely similar, leading to a poor determination of the flow transverse to this line. For this reason the EISCAT Polar experiment was devised to determine the horizontal vector flow far to the north of Tromsø by a beam-swinging technique (van Eyken *et al.* 1984; Willis *et al.* 1986). The beam is directed at a low elevation angle to the north of Tromsø, and periodically swung through a small angle on either side of the L-shell meridian. A range profile of parameters is obtained at the two dwell positions on either side of the meridian where the beam passes through the F-region ionosphere, the flow being determined by pairwise combination of the line-of-sight velocity components. The analysis assumes that the field-parallel flow can be neglected compared with that perpendicular to the field, an assumption which should be valid under most, but not all circumstances (Winser *et al.* 1986, 1988). The advantage of the method is that a detailed latitude profile of the horizontal flow between 70° and 76° invariant latitude is obtained with a few minutes resolution.

In the following section we will present flow observations determined both from tristatic and monostatic measurements with the EISCAT radar.

4. EISCAT MEASUREMENTS IN THE NIGHTSIDE IONOSPHERE

In considering the flow in the nightside ionosphere, and attendant effects on the density and temperature of the ionospheric plasma, two principal influences may be anticipated on the basis of the discussion in §2. The first is the effect of dayside reconnection, which produces a flow which is, to a first approximation, 'directly driven' by IMF B_z, and which appears in the nightside auroral zone with a delay of typically 15 to 20 min, and the second is the effect of

PHILOSOPHICAL TRANSACTIONS OF THE ROYAL SOCIETY A MATHEMATICAL, PHYSICAL & ENGINEERING SCIENCES

rapid tail reconnection (i.e. substorms), which usually appears with a delay of 60 min after an enduring southward turning of the IMF. After such a turning, therefore, 'directly driven' flows should appear after *ca.* 15–20 min, and substorm-associated flows after a further *ca.* 40 min. Both effects will tend to produce equatorward flows in the midnight sector, but the latter should also be accompanied by rapid changes in the ionospheric parameters caused by enhanced electron precipitation, as outlined in the previous section.

The first EISCAT measurements to be discussed were obtained during the Worldwide Atmospheric Gravity Wave Study (WAGS), conducted from 11 to 18 October 1985 (Williams *et al.* 1988). The main thrust of the experiment was to study the generation of large-scale atmospheric gravity waves, but as these are generated by the input of energy and momentum to the atmosphere in the auroral zone, the EISCAT WAGS measurements involved detailed observations of the electrojets. In figure 3*a* we show the *X*-component of magnetograms from the EISCAT magnetometer cross for the period 18h00–06h00 U.T. on the night of 15–16 October 1985. The observations span the range of invariant latitudes from 64.8° (Muonio) to 67.4° (Sørøya), and magnetic local time (MLT) may be found by adding 3h20 to U.T. Two principal substorm sequences can be seen, starting at *ca.* 21h30 and *ca.* 02h10 U.T., upon which considerable shorter-timescale variations are superposed. In each case the disturbance first develops gradually, corresponding to the growth phase, followed 40 min later (at *ca.* 22h10 and 02h50 U.T. respectively) by a sharp increase, which we take to correspond to the start of the expansion phase (though we cannot be categorical about this without examination of auroral and/or Pi2 data). In the case of the first period of disturbance, further sharp changes occur at 20–30 min intervals which appear to be the signatures of multiple onsets. At the top of the plot we also show IMF B_z, as measured by the *International Sun–Earth Explorer* 1 (*ISEE*1) spacecraft in the solar wind. It can be seen that the periods of disturbance are clearly related to intervals of negative IMF B_z, the first initiated by an (interrupted) southward turn shortly before 21h00 U.T., the second by the appearance of strong southward fields after *ca.* 01h50 U.T. Close correspondences can also be seen between shorter-timescale variations in IMF B_z and the magnetic disturbance. In particular, the disturbance enhancements peaking at 23h50, 01h00 and 01h50 U.T. appear to be closely correlated with negative excursions of the IMF appearing 15–20 min earlier, as indicated by the staggered lines. We infer that some or all of these perturbations represent the effect of the flow component which is 'directly driven' by dayside reconnection. Some of the major variations that occur after the inferred onset of the expansion phases do not appear to correspond directly to changes in IMF B_z, however, such as the 'multiple onset' enhancements during the first interval of disturbance, which occur during a period in which (shifted) IMF B_z, while remaining negative, is much smaller than previously. We infer that the corresponding flows are driven mainly by tail reconnection, which begins just over an hour after the first southward turning of the IMF.

In figure 3*b* we show EISCAT data for the 'local' overhead ionosphere, corresponding to an

FIGURE 3. (*a*) Satellite measurements of the interplanetary magnetic field compared with the *X*-component of the data from the EISCAT magnetometer cross on 15–16 October 1985. (Kev is Kevalo, Kil is Kilpisjärvi, Kau is Kautokeino, Muo is Muonio.) (*b*) Satellite measurements of the interplanetary magnetic field compared with EISCAT measurements on 15–16 October 1985 of the north–south, field-perpendicular plasma velocity, the electron temperature at 306 km and the electron concentration at 160 km. (*c*) The spectra of time variations of the north–south field-perpendicular plasma velocity, the electron temperature at 306 km and the electron concentration at 160 km for the interval 21–03h U.T. on 15–16 October 1985.

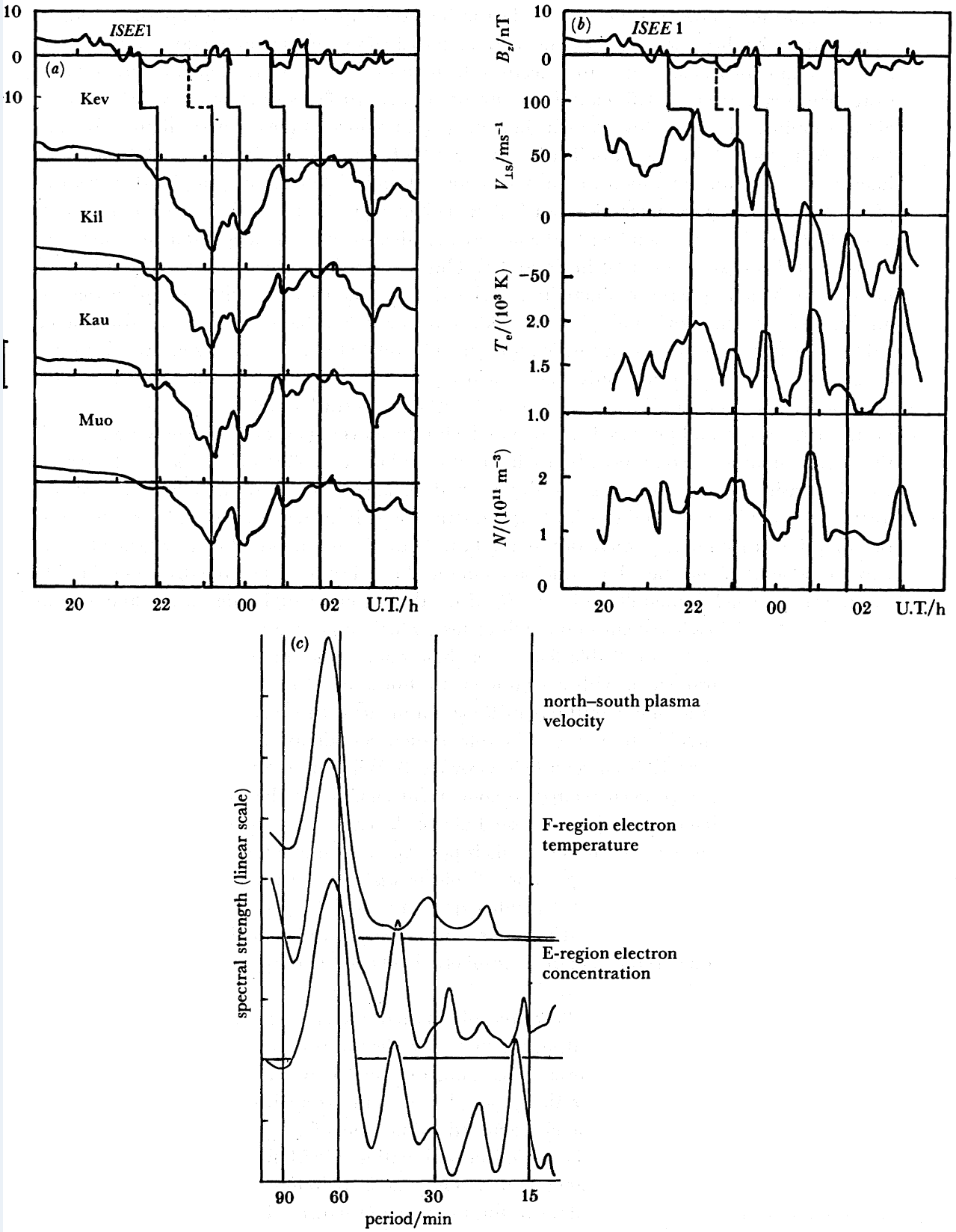

FIGURE 3. For description see opposite.

PHILOSOPHICAL TRANSACTIONS OF THE ROYAL SOCIETY A MATHEMATICAL, PHYSICAL & ENGINEERING SCIENCES

invariant latitude of 67°, specifically $V_{\perp S}$ the southward component of F-region plasma velocity (obtained by the three-point monostatic method described in the previous section), the electron concentration at 160 km, and the electron temperature at 266 km. The first interval of disturbance is associated with continuous strong southward flows starting at *ca.* 21h15 U.T., about 20 min after the southward turn of the IMF (again plotted at the top of the figure). During the growth phase T_e increases, indicating increased soft electron precipitation, while after the inferred onset of the expansion phase N is increased and T_e falls, indicating harder electron precipitation. Both parameters (but not $V_{\perp S}$) are enhanced for an interval of *ca.* 20 min starting at *ca.* 23h00 U.T., corresponding to the largest negative spike in the magnetometer data seen in the first disturbance interval in figure 3*a*. This feature thus appears to correspond to an increase in the ionospheric conductivity associated with enhanced precipitation rather than to an increase in the flow and electric field. On the other hand, the three disturbance enhancements pointed out above which appear to be related to intervals of southward IMF are each associated with a large positive increase in $V_{\perp S}$, together with increases in N or T_e, or both. (In the second and third cases the southward flow perturbation is superposed upon a northward background presumably associated with the morning auroral zone flow.) Similarly, the beginning of the second disturbance interval (starting at *ca.* 02h10 U.T.) is also associated with increasing $V_{\perp S}$, and the onset of the inferred expansion phase at *ca.* 02h50 U.T. with a further increase in $V_{\perp S}$, together with large enhancements in N and T_e, arising from enhanced precipitation. In summary, therefore, the data in figure 3*a*, *b* provide direct evidence for the two components of nightside flow anticipated in the above discussion i.e. that driven by dayside reconnection, which is modulated by IMF B_z with a delay (on the nightside) of 15–20 min, and that driven by nightside reconnection (substorms), which appear after about another 40 min.

Overall, however, a remarkable feature of these data is the quasi-periodic nature of the variations in all parameters, with a characteristic timescale of *ca.* 1 h. Figure 3*c* shows the spectral strength of the time variations in these parameters. In every case there is a peak at *ca.* 65 min which is significant at 1%. The role of such periodicity in generating atmospheric gravity waves has already been reported (Crowley & Williams 1987; Williams *et al.* 1988). Here the variations have been related to concurrent changes in the IMF and in the level of geomagnetic disturbance. The data discussed above clearly indicate that the basic periodicity is already inherent in the IMF, although this is not expressed unmodified in nightside auroral zone flows, because of the superposition of effects associated with dayside and nightside reconnection, which have different dependencies on IMF B_z. The periodicity is also present in the ground magnetometer observations, but is not always so obvious because the magnetic effects depend both on variations in the ionospheric Hall conductivity, as well as on the electric field.

Quasi-periodic variations of the flows and plasma parameters in the nightside auroral zone ionosphere are commonly observed, as we shall now demonstrate by briefly discussing three more examples. Figure 4 also shows WAGS data, obtained between 16h00 and 22h00 U.T. (19h20–01h20 MLT) on 13 October 1985, and plotted in the same format as figure 3*b*. Again, a quasi-periodic variation with a characteristic timescale of *ca.* 1 h is present in all the ionospheric parameters. During the period of observation *ISEE*1 first crossed the bowshock and later (20h30 U.T.) the magnetopause. The IMF is therefore strongly perturbed but examination of the *ISEE*1 IMF B_z data in the top panel of figure 4 indicates that the auroral

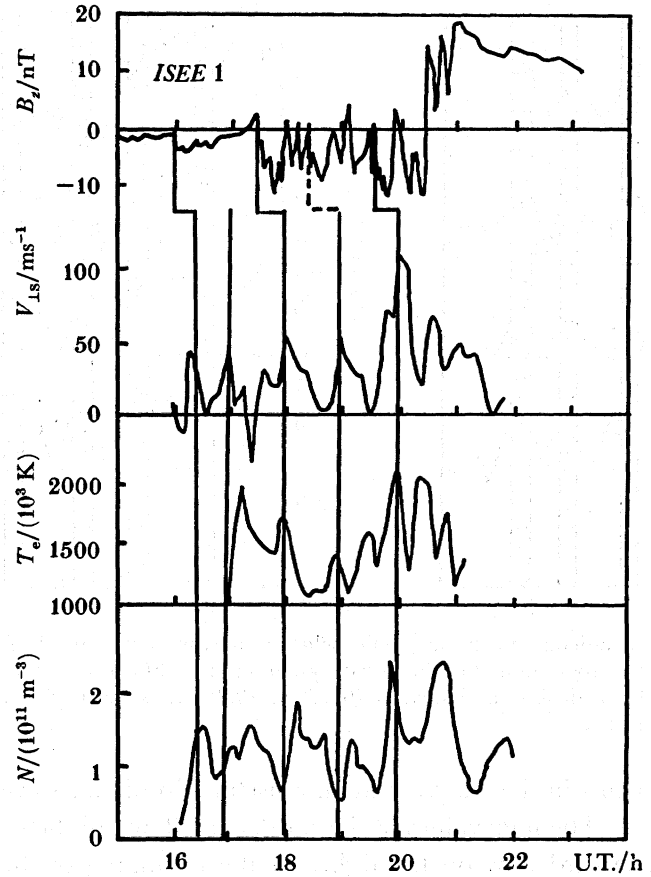

FIGURE 4. Satellite measurements of the interplanetary field inside the bow shock compared with EISCAT measurements on 13 October 1985 of the north–south field-perpendicular plasma velocity, the electron temperature at 306 km and the electron concentration at 160 km.

zone periodicity is again inherent in the interplanetary medium, with very large negative values exceeding −5 nT being intermittently present. Related intervals of strong southward flow, and enhanced N and T_e values, follow with a 15 min delay, as indicated by the staggered lines.

A very clear way of illustrating the relation between plasma velocity, electron temperature and electron concentration is the use of colour contour plots. In figure 5*a*, *b*, plates 1 and 2, ionospheric parameters measured on 26 March 1986 and 18 November 1987 are displayed as colour contours against time and height. The plasma velocity is measured upwards along the magnetic field line, but due to the effects of induced ion drag and diffusion this is highly correlated with the plasma velocity perpendicular to the field line in the north–south direction, so that 'red' contour represent southward bursts of the plasma velocity. It is obvious that these bursts recur in a quasi-periodic manner, and careful examination confirm that the electron temperature in the F-region and the electron concentration below 200 km show a very similar behaviour with southward bursts of plasma velocity corresponding to an increase in electron temperature in the F-region and electron concentration in the E-region.

Another important property of these southward bursts is shown in figure 6, which displays data obtained from a run of EISCAT Common Programme 2 on 21 October 1987. In this programme the Tromsø antenna scans through four positions in a 6 min cycle, and with the

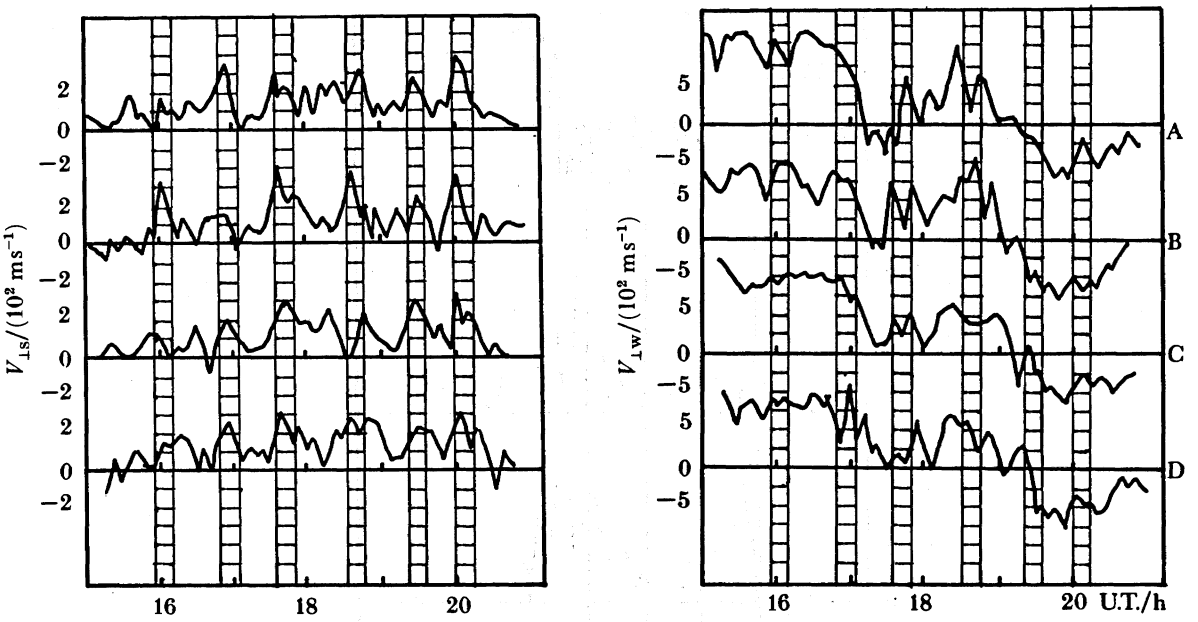

FIGURE 6. Plasma velocity perpendicular to the magnetic field line measured tristatically for the four pointing directions used in Common Programme 2 of the EISCAT system on 21–22 October 1987, showing southward bursts at regular intervals in all four positions: A (69.6° N, 19.2° E); B (69.1° N, 19.2° E); C (68.4° N, 20.0° E); D (68.6° N, 21.9° E).

introduction of improvements in the EISCAT system, a useful tristatic measurement of the flow was obtained at each point. The four values of the southward flow are shown on the left, and the four values of the westward flow on the right. At the beginning of the interval, in the mid-afternoon, the radar observes westward flows of 1 km s^{-1}. Between *ca.* 17h00 and *ca.* 19h00 U.T. the westward flows become more sporadic, and then reverse to eastward, corresponding to a crossing of the Harang discontinuity. In this reversal region the southward flows increase, as expected, but again show the characteristic bursty appearance on timescales of *ca.* 1 h. The large bursts are seen in all four positions, showing that they are features of the flow over a latitude range of at least 1.2° (and also confirming the reliability of the data). The southward bursts are usually accompanied by equally sharp bursts in the other flow component, which are first directed westward, and later eastward, and by a sharp rise in the F-region electron temperature and in the electron density at 160 km.

The last example of this type of behaviour is shown in figure 7, which displays EISCAT Polar data in flow vector format, obtained between 20h30 and 02h30 U.T. (23h00–05h00 MLT) on the night of 3–4 February 1984. A latitude profile of the flow was obtained every 5 min by the two-position beam-swinging technique described in the previous section. (Note that this resolution is half that of the current Polar experiment.) The AE index is plotted at the top of the figure, and shows that the interval was continuously strongly disturbed. AE rarely fell below 500 nT during this period, and showed quasi-periodic enhancements on a timescale of *ca.* 40 min, occasionally reaching 1000–1500 nT. Examination of the Polar data shows that well-defined perturbations of the flow accompany these enhancements, which generally take the form of surges of southward flow, as in the previous examples. Between these surges, and after *ca.* 01h00 U.T. when the AE index shows smoother behaviour, the flows are predominantly eastward, corresponding to the morning auroral zone flow cell.

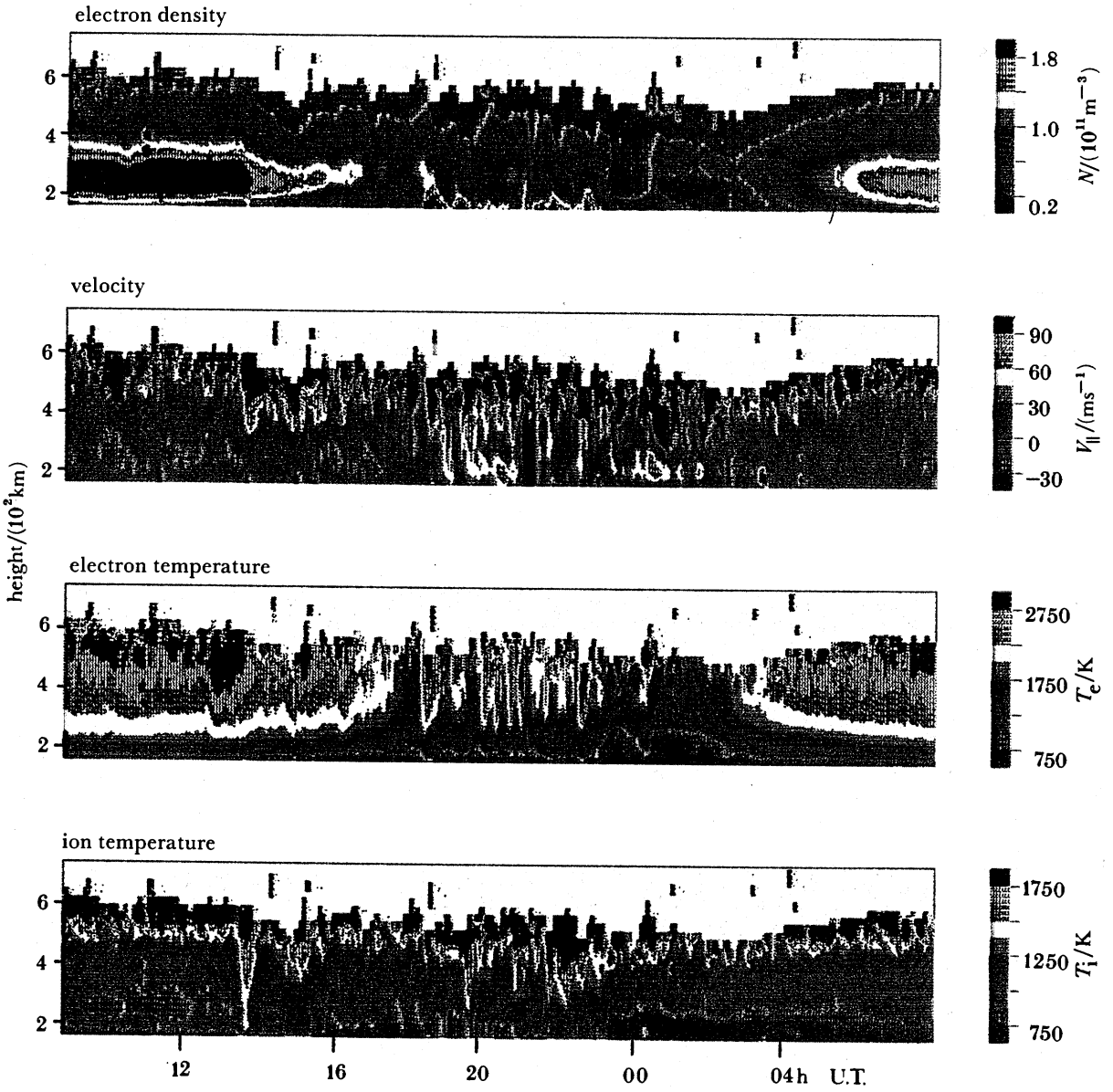

FIGURE 5*a*. EISCAT measurements of electron concentration, field-parallel plasma velocity, electron temperature and ion temperature as functions of height and time for 25–26 March 1986.

(*Facing p.* 186)

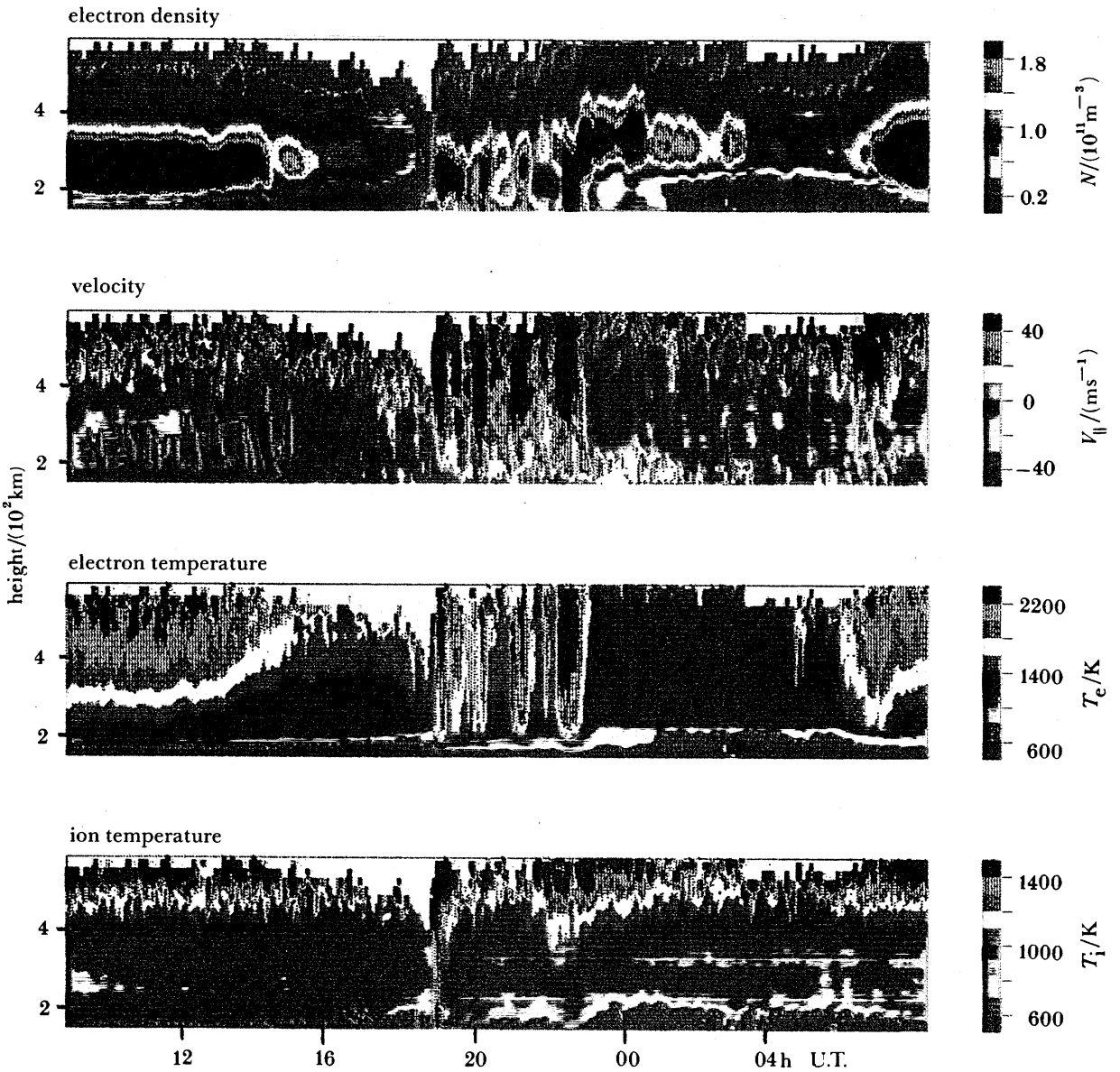

FIGURE 5*b*. EISCAT measurements of electron concentration, field-parallel plasma velocity, electron temperature and ion temperature as functions of height and time for 18–19 November 1987.

PHILOSOPHICAL TRANSACTIONS OF THE ROYAL SOCIETY A MATHEMATICAL, PHYSICAL & ENGINEERING SCIENCES

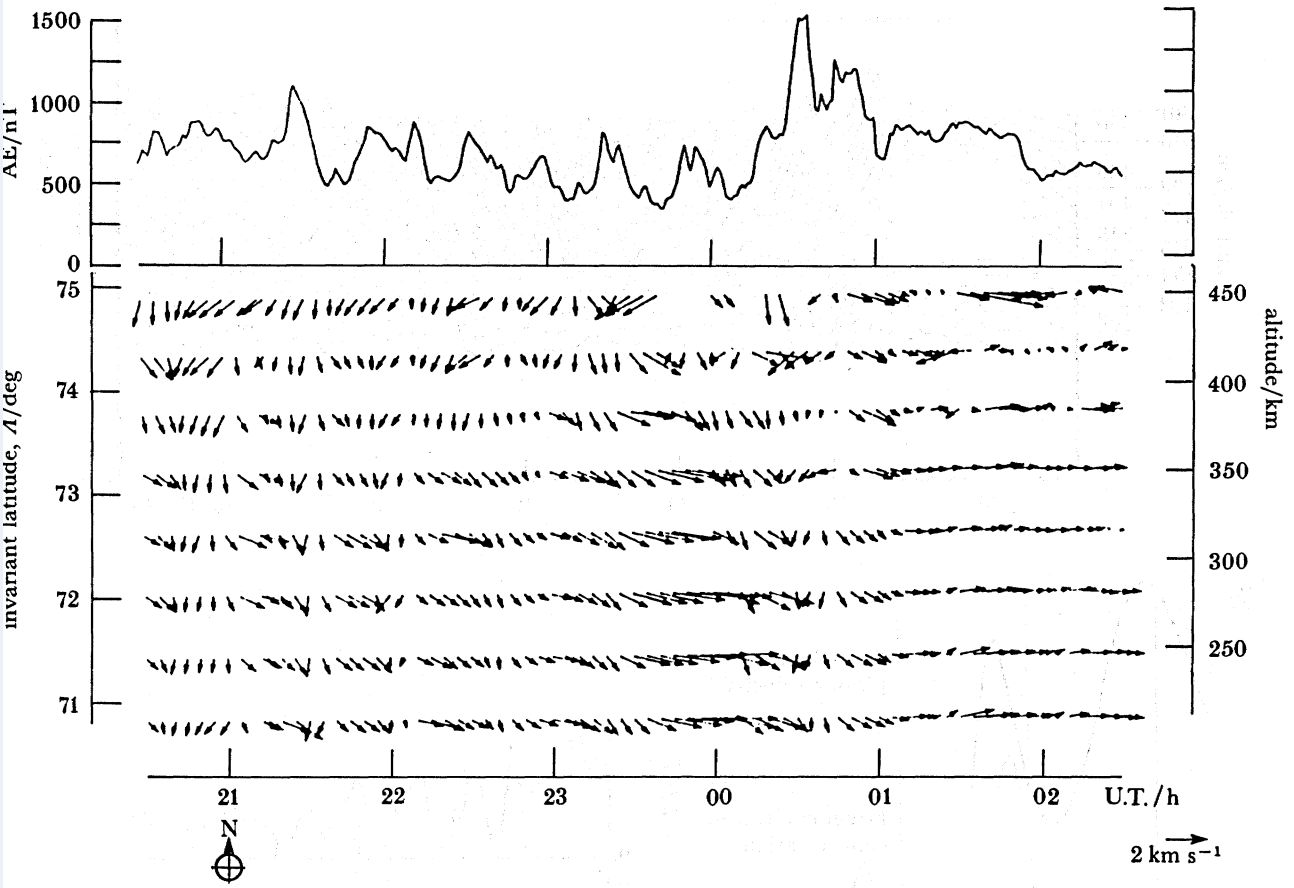

FIGURE 7. The auroral electrojet index AE compared with EISCAT measurements of the vector of field-perpendicular velocity for 3–4 February 1984 using the polar model of observation.

The final data-set to be discussed in this section also provides an example of strong oscillatory behaviour in the disturbed evening to midnight sector of the auroral zone, but it is of a very unusual form and appears to be distinct from the type of variation discussed above. These data were obtained on 18–19 November 1981, when EISCAT was operating in its simplest possible mode, with the Tromsø antenna pointing along the magnetic field line and the remote stations observing at a fixed height of 300 km. Figure 8*a* shows the variation of the electron concentration against height over a 6 h period. A marked oscillation with a $\frac{1}{2}$ h period is evident at F-region heights and in the topside. Figure 8*b* shows the spectra of the variations in the field-aligned plasma velocity, electron concentration and electron temperature for the interval from 16h00 to 21h00 U.T. over a range of heights centred at 500 km. A sharp peak is apparent at 27 min, which is significant at 1%, and also a secondary peak at 54 min. The density oscillation is entirely in phase at all heights, showing that the event is not an atmospheric gravity wave, where we would expect to see a descending phase front. Additionally, on the declining phase of each cycle the timescale of the decrease in electron concentration is much shorter than the ion–electron recombination time at these heights (greater than 1 h). The only realistic interpretation suggests that there were sharp gradients in electron concentration which were swept back and forth through the EISCAT beam by an oscillating electric field. Unfortunately, because of a fault in the receiver at Kiruna it was impossible to measure the full

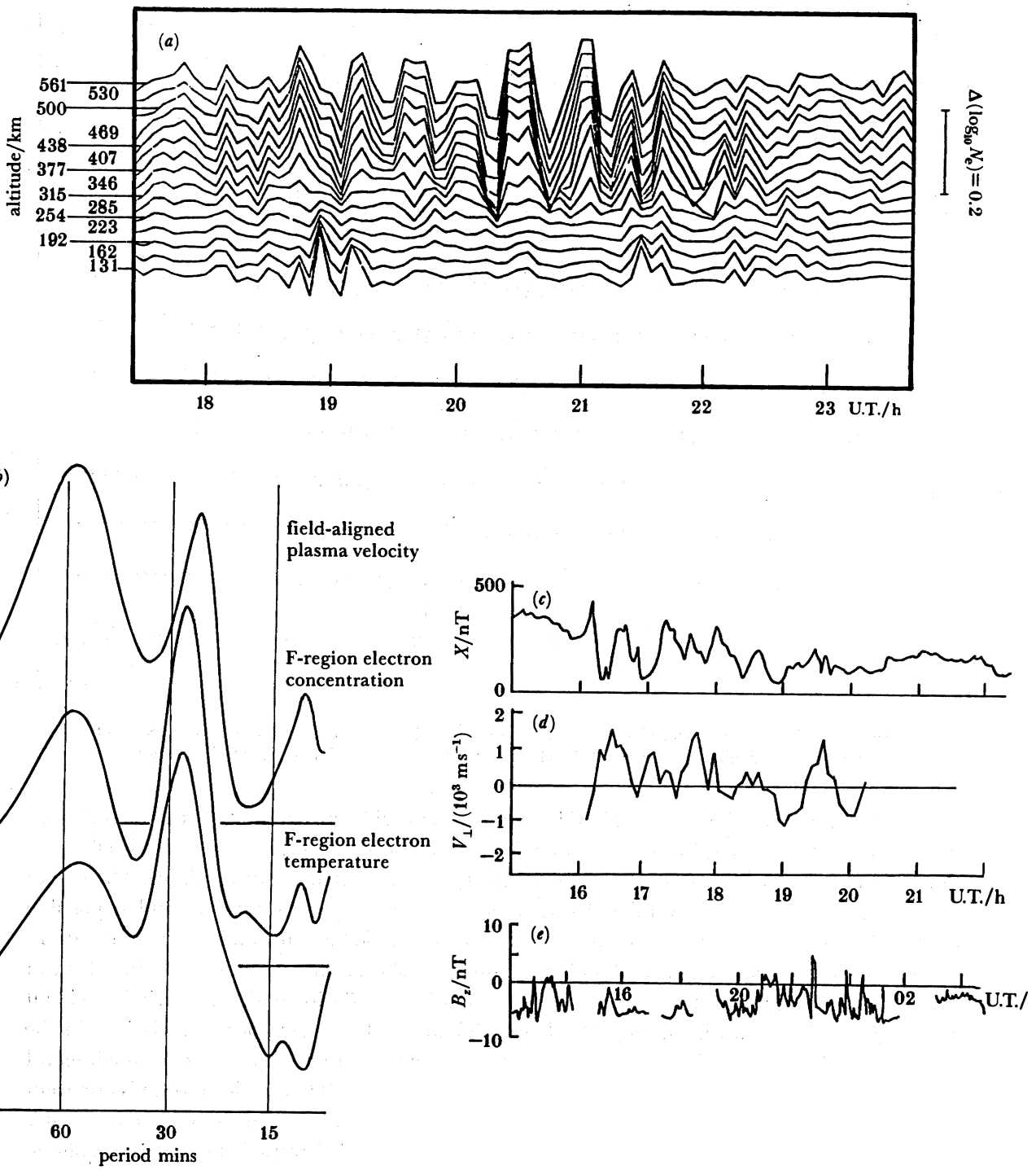

FIGURE 8. (*a*) The variation of electron concentration with height and time on 18 November 1981 (I. T. Price, personal communication). (*b*) The spectra of time variations of field-aligned plasma velocity, electron concentration and electron temperature over the height range 460–540 km for the interval 16–21h U.T. on 18 November 1981. (*c*) The *X*-component of the magnetometer data from Tromsø on 18 November 1981. (*d*) The measured plasma velocity perpendicular to the magnetic field line and lying in the plane defined by the antenna beams at Tromsø and Sodankylä on 18 November 1981. (*e*) B_z-component of the interplanetary field as measured by *ISEE*3 on 18–19 November 1981.

vector flow, but it was possible to measure one component of the flow transverse to the field from measurements at Sodankylä, as shown in figure 8*c*. This shows an oscillating flow with an amplitude as large as 1.5 km s^{-1} and a period of *ca.* 50 min. There is good agreement between the times when this component of velocity shows a reversal and when the electron concentration shows a minimum, which is consistent with our interpretation in terms of an oscillating spatial boundary.

It is instructive to compare the EISCAT results with the magnetometer data obtained at Tromsø (figure 8*d*). Between 16h00 and 18h00 U.T. the *X*-component shows a basic cycle at 55 min, with a clear harmonic at 27 min, but this dies away after 19h00 U.T. when EISCAT registers the strongest oscillation. This apparent discrepancy is resolved when the EISCAT E-region echoes are examined. Between 16h00 and 18h00 U.T. the E-region concentration was large, such that both the Hall and Pedersen currents were also large. After 18h00 U.T. the electron population below 150 km effectively disappeared, but above 150 km it is unchanged, so that although the Hall current is much smaller, the Pedersen current continues.

Finally, in figure 8*e* we show concurrent variations in IMF B_z, measured at the upstream Lagrangean point by the *ISEE*3 spacecraft. The time delay to the Earth is *ca.* 1 h. It can be seen that the IMF was nearly continuously strongly southward during this period, but gives no indication in this case of an oscillation corresponding to that observed by EISCAT. For example, IMF B_z was very steady at *ISEE*3 during the interval 16h00–17h00 U.T., while during the corresponding interval at EISCAT (*ca.* 17h00–18h00 U.T.) strong oscillations were observed.

5. Summary and discussion

In this paper we have reviewed current understanding of the magnetospheric substorm phenomenon, with emphasis on the relation between space-based and ground-based observations. It seems clear that most relevant data can be understood in terms of the picture in which a new neutral line forms in the near-Earth plasma sheet at substorm expansion phase onset, following a period of tail development (growth) associated with negative IMF B_z, and then moves rapidly tailward during substorm recovery. In this picture, the flow in the nightside auroral zone ionosphere should consist of two basic components. The first is associated with dayside reconnection, 'directly driven' by southward IMF B_z, which expands from the noon dayside sector and reaches the nightside with a delay of 15–20 min. The other is associated with rapid tail reconnection during substorms, which typically begins about one hour after southward turns of the IMF. Examination of recent EISCAT, ground-based magnetometer and IMF measurements provides evidence for the influence of both components in the nightside high-latitude ionosphere.

These studies have also revealed the presence of a new qualitative property of nightside auroral zone flows and ionospheric plasma parameters, that they commonly vary in a quasi-periodic fashion with a typical period of 1 h. The characteristic feature is an equatorward surge of the plasma, often accompanied by an increase in E-region electron concentration, or by an increase in F-region electron temperature, or both. A similar periodicity is often suggested in magnetometer records, but the perturbation magnetic field depends not only on the flow, but also on the E-region electron concentration below 130 km (i.e. on the Hall conductivity), and the EISCAT data confirm that this varies more sporadically. On the other hand, the electron concentration at greater heights, which controls the Pedersen conductivity and Joule dissipation, is less variable. In two cases where concurrent IMF data are available, it seems clear

PHILOSOPHICAL TRANSACTIONS OF THE ROYAL SOCIETY A MATHEMATICAL, PHYSICAL & ENGINEERING SCIENCES

that the observed periodicity is already inherent in IMF B_z, but it is not expressed unmodified in the nightside flows, because of the presence of the two flow components mentioned above which depend on IMF B_z in different ways. We have examined about 20 nightside data intervals, and although the pattern is not always as regular as in the examples given above, the basic features can be recognized in most cases. Observed periods range from 35 to 70 min or more, but for the large majority of cases the cycle time is *ca.* 60 min.

The next step is to catalogue all examples of quasi-periodic behaviour observed by EISCAT, and compare these results with measurements of the IMF. Looking further to the future, we anticipate a major step will be taken when coordinated multipoint observations become available, by using EISCAT to monitor the nightside ionosphere, while spacecraft in the solar wind monitor the IMF, and spacecraft in the tail (e.g. *Cluster*) observe the behaviour of the plasma sheet.

The authors thank the Director and Staff of EISCAT for the incoherent-scatter data used in this paper. EISCAT is an international facility supported by Finland, France, Germany, Norway, Sweden and the United Kingdom. We thank the EISCAT group at the Rutherford Appleton Laboratory for substantial help in processing these data. We also acknowledge with gratitude the access to data from *ISEE*1 and the EISCAT Magnetometer Cross.

REFERENCES

Aggson, T. L., Heppner, J. P. & Maynard, N. C. 1983 *J. geophys. Res.* **88**, 3981–3990.
Akasofu, S.-I. 1964 *Planet. Space Sci.* **12**, 273–282.
Arnoldy, R. L. & Chan, K. W. 1969 *J. geophys. Res.* **74**, 5019–5028.
Arnoldy, R. L. & Moore, T. E. 1983 *J. geophys. Res.* **88**, 6213–6220.
Atkinson, G., Crentzberg, F., Gattinger, R. L. & Murphee, J. S. 1988 Preprint, Hertzberg Institute of Astrophysics.
Aubry, M. P., Russell, C. T. & Kivelson, M. G. 1970 *J. geophys. Res.* **75**, 7018–7031.
Baker, D. N., Higbie, P. R., Hones, E. W. Jr & Belian, R. D. 1978 *J. geophys. Res.* **83**, 4863–4868.
Baker, D. N., Belian, R. D., Higbie, P. R. & Hones, E. W. Jr 1979 *J. geophys. Res.* **4**, 7138–7154.
Baker, D. N., Fritz, T. A., Wilken, B., Higbie, P. R., Kaye, S. M., Kivelson, M. G., Moore, T. E., Studemann, W., Masley, A. J., Smith, P. H. & Vampola, A. L. 1982 *J. geophys. Res.* **87**, 5917–5932.
Baker, D. N., Bame, S. J., Belian, R. D., Feldman, W. C., Gosling, J. T., Higbie, P. R., Hones, E. W. Jr, McComas, D. J. & Zwickl, R. D. 1984*a* *J. geophys. Res.* **89**, 3855–3864.
Baker, D. N., Akasofu, S.-I., Baumjohann, W., Bieber, J. W., Fairfield, D. H., Hones, E. W. Jr, Mauk, B. H., McPherron, R. L. & Moore, T. E. 1984*b* In *Solar–terrestrial physics – past and future* (NASA Pub. no. 1120), p. 8-1. Washington, D.C.
Baker, D. N., Fritz, T. A., McPherron, R. L., Fairfield, D. H., Kamide, Y. & Baumjohann, W. 1985 *J. geophys. Res.* **90**, 1205–1216.
Baker, D. N., Anderson, R. C., Zwickl, R. D. & Slavin, J. A. 1987*a* *J. geophys. Res.* **92**, 71–81.
Baker, D. N., Bame, S. J., McComas, D. J., Zwickl, R. D., Slavin, J. A. & Smith, E. J. 1987*b* In *Magnetotail physics* (ed. A. T. Y. Lui), p. 137. Baltimore: JHU Press.
Banks, P. M. 1977 *J. atmos. terr. Phys.* **39**, 179–193.
Bargatze, L. F., Baker, D. N., McPherron, R. L. & Hones, E. W. Jr 1985 *J. geophys. Res.* **90**, 6387–6394.
Baumjohann, W. 1986 *J. Geomagn Geoelect., Kyoto* **38**, 633–652.
Baumjohann, W. 1988 *J. Geomagn Geoelect., Kyoto* **40**, 157–176.
Baumjohann, W., Pellinen, R. J., Opgenoorth, H. J. & Nielsen, E. 1981 *Planet. Space Sci.* **29**, 431–447.
Bieber, J. W., Stone, E. C., Hones, E. W. Jr, Baker, D. N. & Bame, S. J. 1982 *Geophys. Res. Lett.* **9**, 664–667.
Boström, R. 1964 *J. geophys. Res.* **69**, 4983–4999.
Boström, R. 1974 In *Magnetospheric physics* (ed. B. M. McCormac), pp. 45–59. Hingham, Massachusetts: Reidel.
Buck, R. M., West, H. I. Jr & D'Arcy, R. G. 1973 *J. geophys. Res.* **78**, 3103–3118.
Caan, M. N., McPherron, R. L. & Russell, C. T. 1978 *Planet. Space Sci.* **26**, 269–279.
Clauer, C. R. & McPherron, R. L. 1974 *J. geophys. Res.* **79**, 2811–2820.
Coroniti, F. V., Frank, L. A., Williams, D. A., Lepping, R. P., Scarf, F. L., Krimigis, S. M. & Gloeckler, G. 1980 *J. geophys. Res.* **85**, 2957–2977.

PHILOSOPHICAL TRANSACTIONS OF THE ROYAL SOCIETY A MATHEMATICAL, PHYSICAL & ENGINEERING SCIENCES

Craven, J. D. & Frank, L. A. 1987 *J. geophys. Res.* **92**, 4565–4573.
Crowley, G. & Williams, P. J. S. 1987 *Nature, Lond.* **328**, 231–233.
Cummings, W. D., Barfield, J. N. & Coleman, P. J. Jr 1968 *J. geophys. Res.* **73**, 6687–6698.
DeForest, S. E. & McIlwain, C. E. 1971 *J. geophys. Res.* **76**, 3587–3611.
Etemadi, A., Cowley, S. W. H., Lockwood, M., Bromage, B. J. I., Willis, D. M. & Lühr, H. 1988 *Planet. Space Sci.* **36**, 471–498.
van Eyken, A. P., Rishbeth, H., Willis, D. M. & Cowley, S. W. H. 1984 *J. atmos. terr. Phys.* **46**, 635–641.
Fairfield, D. H. 1971 *J. geophys. Res.* **76**, 6700–6716.
Fairfield, D. H. 1986 *J. geophys. Res.* **91**, 4238–4244.
Fairfield, D. H., Hones, E. W. Jr & Meng, C.-I. 1981 *J. geophys. Res.* **86**, 11189–11200.
Fairfield, D. H., Baker, D. N., Craven, J. D., Elphic, R. C., Fennell, J. F., Frank, L. A., Richardson, I. G., Singer, H. J., Slavin, J. A., Tsurutani, B. T. & Zwickl, R. D. 1989 *J. geophys. Res.* (In the press.)
Folkestad, K., Hagfors, T. & Westerlund, S. 1983 *Radio Sci.* **18**, 867–879.
Galeev, A. A., Coroniti, F. V. & Ashour-Abdalla, M. 1978 *Geophys. Res. Lett.* **5**, 707–714.
Holzer, R. E. & Slavin, J. A. 1978 *J. geophys. Res.* **83**, 3831–3839.
Holzer, R. E., McPherron, R. L. & Hardy, D. A. 1986 *J. geophys. Res.* **91**, 3287–3293.
Hones, E. W. Jr 1973 *Radio Sci.* **8**, 979–990.
Hones, E. W. Jr 1979 *Space Sci. Rev.* **23**, 393–410.
Hones, E. W. Jr, Akasofu, S.-I., Bame, S. J. & Singer, S. 1971 *J. geophys. Res.* **76**, 8241–8257.
Hones, E. W. Jr, Ashbridge, J. R., Bame, S. J. & Singer, S. 1973 *J. geophys. Res.* **78**, 109–132.
Hones, E. W. Jr, Bame, S. J. & Ashbridge, J. R. 1976 *J. geophys. Res.* **81**, 227–234.
Hones, E. W. Jr, Baker, D. N., Bame, S. J., Feldman, W. C., Gosling, J. T., McComas, D. J., Zwickl, R. D., Slavin, J. A., Smith, E. J. & Tsurutani, B. T. 1984*a* *Geophys. Res. Lett.* **11**, 5–7.
Hones, E. W. Jr, Birn, J., Baker, D. N., Bame, S. J., Feldman, W. C., McComas, D. J. & Zwickl, R. D. 1984*b* *Geophys. Res. Lett.* **11**, 1046–1049.
Horwitz, J. L. 1985 *J. geophys. Res.* **90**, 4164–4170.
Inhester, B. W., Baumjohann, W., Greenwald, R. A. & Nielsen, E. 1981 *J. Geophys.* **49**, 155–170.
Jones, G. O. L., Winser, K. J. & Williams, P. J. S. 1986 *J. atmos. terr. Phys.* **48**, 887–892.
Kivelson, M. G., Farley, T. A. & Aubry, M. P. 1973 *J. geophys. Res.* **78**, 3079–3092.
Kokubun, S., McPherron, R. L. & Russell, C. T. 1977 *J. geophys. Res.* **82**, 74–86.
Lockwood, M., van Eyken, A. P., Bromage, B. J. I., Willis, D. M. & Cowley, S. W. H. 1986 *Geophys. Res. Lett.* **13**, 72–75.
Lopez, R. E., Lui, A. T. Y., Sibeck, D. G., McEntire, R. W., Zanetti, L. J., Potemra, T. A. & Krimigis, S. M. 1988 *J. geophys. Res.* **93**, 997–1001.
Lui, A. T. Y., Hones, E. W. Jr, Venkatesan, D., Akasofu, S.-I. & Bame, S. J. 1975 *J. geophys. Res.* **80**, 4649–4659.
Maezawa, K. 1975 *J. geophys. Res.* **80**, 3543–3548.
Mauk, B. H. 1986 *J. geophys. Res.* **91**, 13423–13454.
Mauk, B. H. & Meng, C.-I. 1983 *J. geophys. Res.* **88**, 3055–3071.
McPherron, R. L. 1970 *J. geophys. Res.* **75**, 5592–5599.
McPherron, R. L. 1972 *Planet. Space Sci.* **20**, 1521–1539.
McPherron, R. L. 1979 *Rev. Geophys. Space Phys.* **17**, 657–681.
McPherron, R. L., Russell, C. T. & Aubry, M. P. 1973 *J. geophys. Res.* **78** 3131–3149.
Moore, T. E., Arnoldy, R. L., Feynmann, J. & Hardy, D. A. 1981 *J. geophys. Res.* **86**, 6713–6726.
Morozumi, H. M. 1965 *Rep. Ionos. Space Res. Jap.* **19**, 286–298.
Nagai, T. 1987 *J. geophys. Res.* **92**, 2432–2446.
Nagai, T., Baker, D. N. & Higbie, P. R. 1983 *J. geophys. Res.* **88**, 6994–7004.
Nishida, A. 1968*a* *J. geophys. Res.* **73**, 1795–1803.
Nishida, A. 1968*b* *J. geophys. Res.* **73**, 5549–5559.
Nishida, A. & Nagayama, N. 1973 *J. geophys. Res.* **78**, 3782–3798.
Paschmann, G., Papamastorakis, I., Baumjohann, W., Sckopke, N., Carlson, C. W., Sonnerup, B. U. O. & Lühr, H. 1986 *J. geophys. Res.* **91**, 11099–11115.
Pedersen, A., Grard, R., Knott, K., Jones, D. & Gonfalone, A. 1978 *Space Sci. Rev.* **22**, 333–346.
Pytte, T., McPherron, R. L. & Kokubun, S. 1976*a* *Planet. Space Sci.* **24**, 1115–1132.
Pytte, T., McPherron, R. L., Kivelson, M. G., West, H. I., Jr & Hones, E. W. Jr 1976*b* *J. geophys. Res.* **81**, 5921–5933.
Pytte, T., McPherron, R. L., Hones, E. W. Jr & West, H. I. Jr 1978 *J. geophys. Res.* **83**, 663–679.
Quinn, J. M. & McIlwain, C. E. 1979 *J. geophys. Res.* **84**, 7365–7370.
Quinn, J. M. & Southwood, D. J. 1982 *J. geophys. Res.* **87**, 10536–10540.
Richardson, I. G. & Cowley, S. W. H. 1985 *J. geophys. Res.* **90**, 12133–12158.
Richardson, I. G. & Cowley, S. W. H. 1987 In *Magnetotail physics* (ed. A. T. Y. Lui). Baltimore: JHU Press.
Richardson, I. G., Scholer, M., Tsurutani, B. T., Daly, P. W., Baker, D. N. & Elphic, R. C. 1987*a* *Planet. Space Sci.* **35**, 209–226.

PHILOSOPHICAL TRANSACTIONS OF THE ROYAL SOCIETY A MATHEMATICAL, PHYSICAL & ENGINEERING SCIENCES

Richardson, I. G., Cowley, S. W. H., Hones, E. W. Jr & Bame, S. J. 1987*b* *J. geophys. Res.* **92**, 9997–10013.
Richardson, I. G., Owen, C. I., Cowley, S. W. H., Galvin, A. B., Sanderson, T. R., Scholer, M., Slavin, J. A. & Zwickl, R. D. 1989 *J. geophys. Res.* (In the press.)
Rijnbeek, R. P., Cowley, S. W. H., Southwood, D. J. & Russell, C. T. 1984 *J. geophys. Res.* **89**, 786–800.
Rishbeth, H., Smith, P. R., Cowley, S. W. H., Willis, D. M., van Eyken, A. P., Bromage, B. J. I. & Crothers, S. R. 1985 *Nature, Lond.* **318**, 451–452.
Rostoker, G. 1968 *J. geophys. Res.* **73**, 4217–4229.
Rostoker, G. 1983 *J. geophys. Res.* **88**, 6981–6993.
Rostoker, G. & Eastman, T. G. 1987 *J. geophys. Res.* **92**, 12187–12201.
Russell, C. T. & McPherron, R. L. 1973 *Space Sci. Rev.* **15**,. 205–266.
Saito, T. 1969 *Space Sci. Rev.* **10**, 319–412.
Sauvaud, J.-A. & Winckler, J. R. 1980 *J. geophys. Res.* **85**, 2043–2056.
Schlegel, K. & McCrea, I. 1987 Max-Planck-Institut für Aeronomie, Publication W-05-87-05.
Schindler, K. 1974 *J. geophys. Res.* **79**, 2803–2810.
Scholer, M., Gloeckler, G., Klecker, B., Ipavich, F. M., Hovestadt, D. & Smith, E. J. 1984*a* *J. geophys. Res.* **89**, 6717–6727.
Scholer, M., Gloeckler, G., Hovestadt, D., Klecker, B. & Ipavich, F. M. 1984*b* *J. geophys. Res.* **89**, 8872–8876.
Schunk, R. W. & Nagy, A. F. 1978 *Rev. Geophys. Space Phys.* **16**, 355–399.
Shepherd, G. G., Bostrom, R., Derblom, H., Falthammar, C.-E., Gendrin, R., Aila, K., Korth, A., Pedersen, A., Pellinen, R. & Wrenn, G. 1980 *J. geophys. Res.* **85**, 4587–4601.
Singer, H. J., Hughes, W. J., Gelpi, C. & Ledley, B. G. 1985 *J. geophys. Res.* **90**, 9583–9589.
Slavin, J. A., Smith, E. J., Sibeck, D. G., Baker, D. N., Zwickl, R. D. & Akasofu, S.-I. 1985 *J. geophys. Res.* **90**, 10875–10895.
Todd, H., Cowley, S. W. H., Lockwood, M., Willis, D. M. & Lühr, H. 1988 *Plant. Space Sci.* **36**, 1415–1428.
Vorobjev, V. G., Starkov, G. V. & Feldstein, Y. I. 1976 *Planet. Space Sci.* **24**, 955–965.
Williams, P. J. S., Jones, G. O. L. & Jain, A. R. 1984 *J. atmos. terr. Phys.* **46**, 521–530.
Williams, P. J. S., Crowley, G., Schlegel, K., Virdi, T. S., McCrea, I., Watkins, G., Wade, N., Hargreaves, J. K., Lachlan-Cope, T., Muller, H., Baldwin, J. E., Warner, P., van Eyken, A. P., Hapgood, M. A. & Rodger, A. S. 1988 *J. atmos. terr. Phys.* **50**, 323–338.
Willis, D. M., Lockwood, M., Cowley, S. W. H., van Eyken, A. P., Bromage, B. J. I., Rishbeth, H., Smith, P. R. & Crothers, S. R. 1986 *J. atmos. terr. Phys.* **48**, 987–1008.
Winser, K. J., Jones, G. O. L. & Williams, P. J. S. 1986 *J. atmos. terr. Phys.* **48**, 893–904.
Winser, K. J., Jones, G. O. L. & Williams, P. J. S. 1988 *J. atmos. terr. Phys.* **50**, 379–382.

Discussion

M. Lockwood (*Rutherford Appleton Laboratory, Chilton, U.K.*). The recurrence period of substorms that Dr Williams has reported in this paper is very similar to the response time of the DP1 current system (often quantified by the AE index) to changes in the IMF. Is there any evidence in these EISCAT data that the growth phase and spacing of substorms vary with the total energy deposited in the substorms for those cases when the IMF is stable and the substorms are not triggered externally?

P. J. S. Williams. The majority of cases show a recurrence period of *ca.* 60 min. For the 1981 November 18 event, B_z was strongly negative for many hours, and the total energy deposited was very high, but the basic period was 54 min. I would have expected that when the energy input was constant and high the recurrence period would be shorter, but this does not seem to be the case. Our next step is to compare the whole set of examples with IMF measurements to see if there is any correlation between the Akasofu ϵ parameter, or the solar wind velocity, with the recurrence period.

P. Rothwell (*University of Sussex, U.K.*). The EISCAT beam is very narrow (1–2 km in the lower ionosphere) and the auroral ionosphere can be highly structured on this scale in some regions.

Could not the wavelike structures in ion velocity and electron temperature seen by EISCAT be a localized spatial effect, rather than a larger-scale temporal effect?

P. J. S. WILLIAMS. Before 1987 this was a problem. We had a choice of making observations in a fixed direction, when we could not distinguish spatial and temporal effects; or we could scan the Tromsø antenna, but then the signal-to-noise ratio was too low to get reliable velocity measurements from any one position.

Since 1987 the installation of cooled GaAs field-effect transistors at EISCAT have so improved signal-to-noise that in the Common Programme CP2 we can measure plasma velocity in each of four positions in a 6 min cycle. The results from 21–22 October 1987 show a series of southward plasma bursts coinciding in all four positions and lasting for *ca.* 10 min. In other words simultaneous southward bursts plus F-region electron heating occur over a north–south distance of at least 160 km.

K. J. WINSER (*Rutherford Appleton Laboratory, Chilton, U.K.*). It is perfectly true that, in the steady-state or quasi-steady-state conditions, the Joule heating will be overestimated as a result of the exclusion of neutral winds in the calculations. However, during impulsive events when the electric fields can rapidly change direction by 180°, such as were presented in Dr Williams' talk, it is likely that the Joule heating rates will be significantly underestimated.

My comments indicate the importance of simultaneous *ion* and *neutral* measurements to properly assess the role of Joule heating in providing an impulsive source to periodicities in the ionosphere.

P. J. S. WILLIAMS. In the WAGS experiment we did measure plasma velocity in the E-region to estimate the neutral velocity. This is usually possible for heights up to 120 km, but during periods of large electric fields the uncertainty in neutral collision frequency makes any estimate of neutral wind velocity uncertain above 120 km and impossible above 130 km, so for these heights we have to estimate the neutral velocity by modelling. In any case, when we have large, oscillating electric fields the error in Joule heating estimate is small.

PHILOSOPHICAL TRANSACTIONS OF THE ROYAL SOCIETY A MATHEMATICAL, PHYSICAL & ENGINEERING SCIENCES

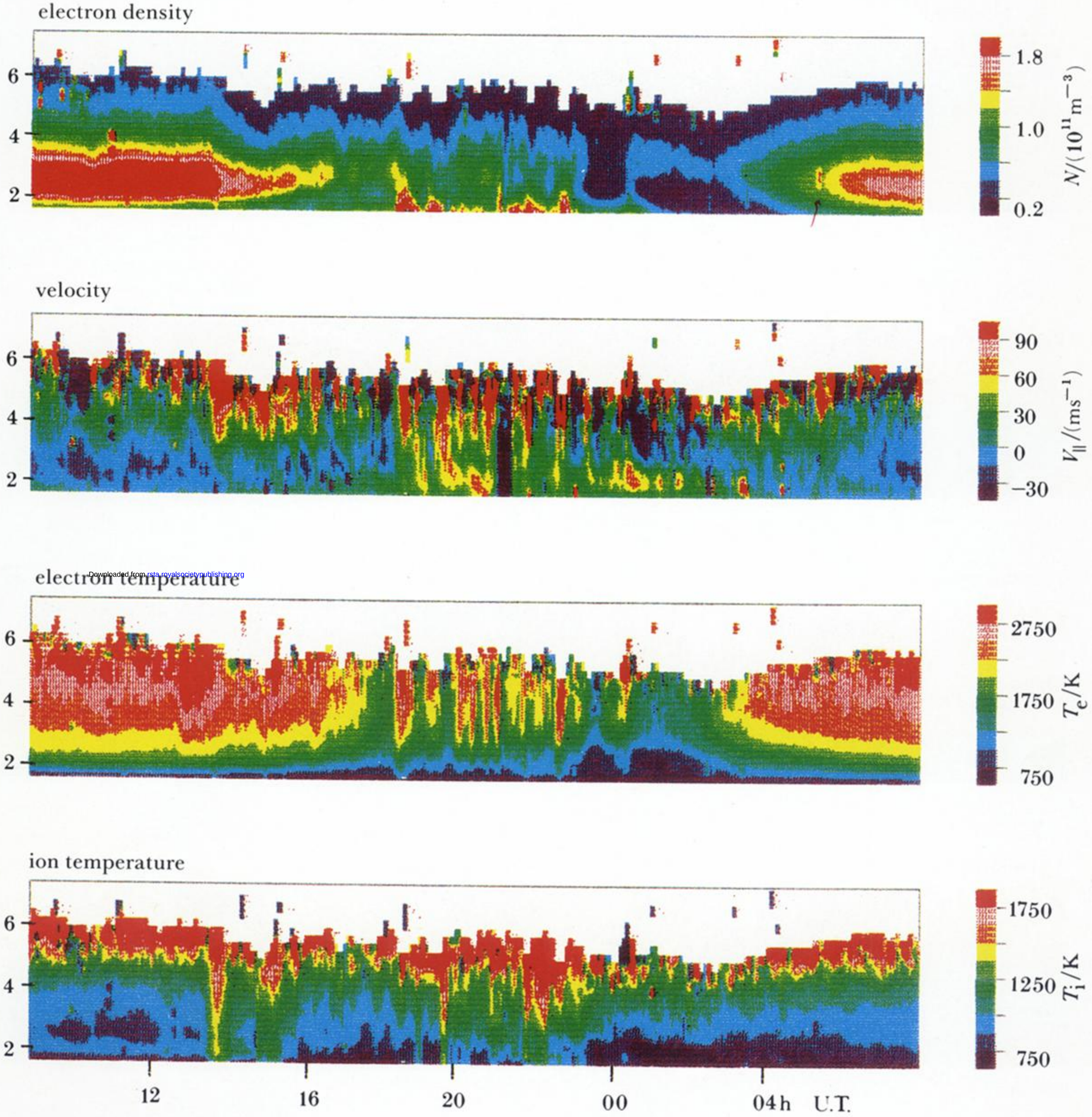

FIGURE 5*a*. EISCAT measurements of electron concentration, field-parallel plasma velocity, electron temperature and ion temperature as functions of height and time for 25–26 March 1986.

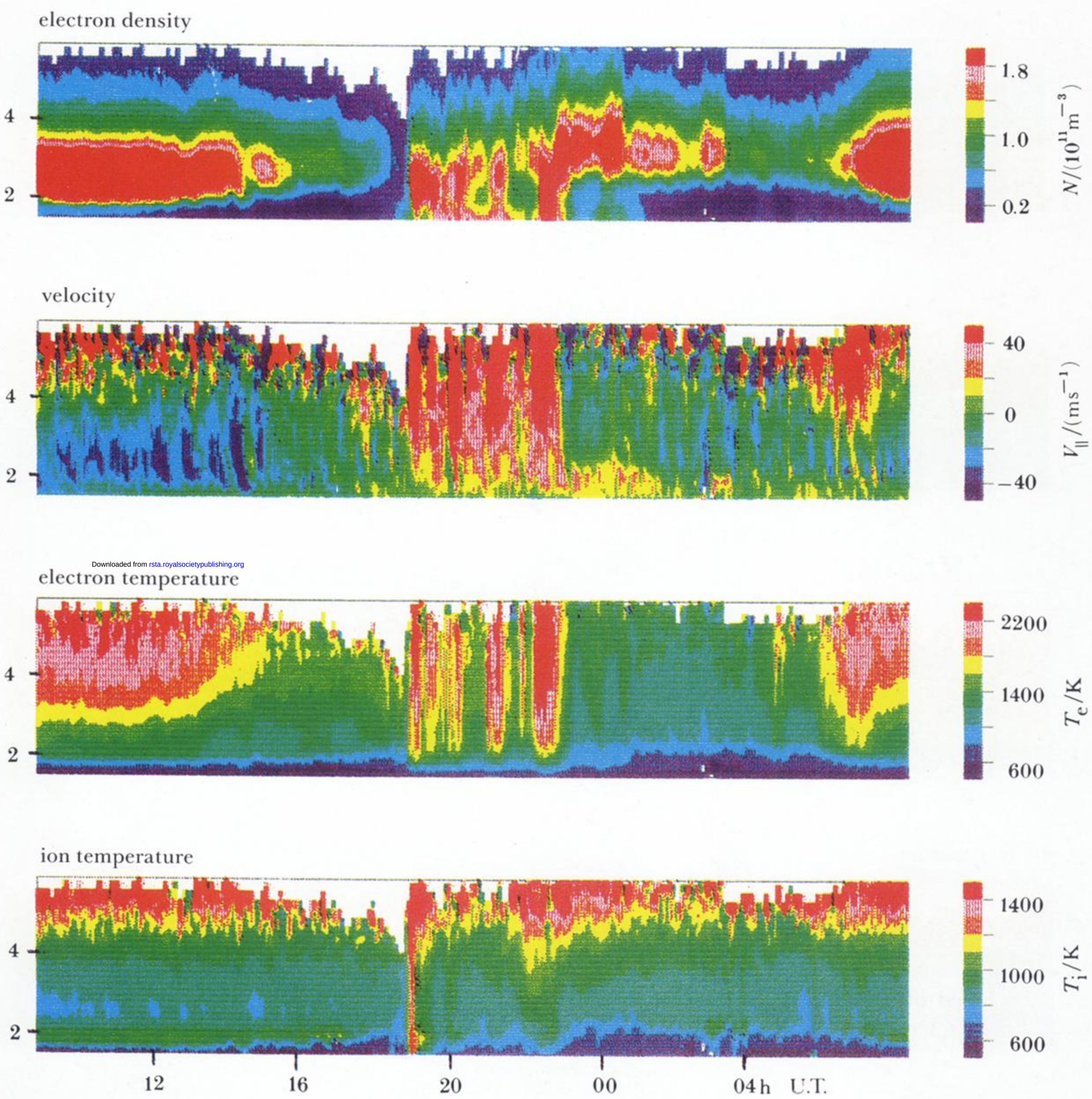

FIGURE 5*b*. EISCAT measurements of electron concentration, field-parallel plasma velocity, electron temperature and ion temperature as functions of height and time for 18–19 November 1987.